Physica D 477 (2025) 134733

Contents lists available at ScienceDirect

Physica D: Nonlinear Phenomena

journal homepage: www.elsevier.com/locate/physd

Analysis of power law behavior of local cortical neurodynamics

Karolina Armonaite [a,b,c], Livio Conti [a,c,*], Marco Balsi [d], Luca Paulon [b], Franca Tecchio [b]

[a] Faculty of Engineering, Uninettuno University, 00186, Rome, Italy
[b] Laboratory of Electrophysiology for Translational NeuroScience, Institute of Cognitive Sciences and Technologies – Consiglio Nazionale delle Ricerche, 00185, Rome, Italy
[c] INFN – Istituto Nazionale di Fisica Nucleare, Sezione Roma Tor Vergata, 00133, Rome, Italy
[d] Department of Information Engineering, Electronics and Telecommunications, Sapienza University, 00184, Rome, Italy

ARTICLE INFO

Keywords:
Intracranial electroencephalography
Power-law
Cortical parceling
Scale-free dynamics

ABSTRACT

Growing evidence suggests that neuronal electrical activity, the neurodynamics, contains specific signatures for distinct cortical parcels of the brain, potentially enabling cortex classification based on it, even in resting states. However, existing algorithms for extracting specific characteristics may succeed only in specific cases, or well selected groups, but often fail to identify stable features across the general populations. Our study examines intracranial stereotactic-electroencephalographic (sEEG) recordings, assessing power-law behavior in power spectral density during wakefulness and sleep stages across three gyri: precentral, postcentral and superior temporal, in 55 subjects. Results indicate the presence of a power-law behavior, implying scale-free dynamics in investigated areas. Notably, power-law exponent in high frequency range distinguishes cortical parcels both in wakefulness and sleep and suggests a stable scale-free pattern within each region possibly regardless of the state. This insight offers valuable guidance for evaluating physiological aspects of local neurodynamics and supports population-level functional cortex parceling.

1. Introduction

Many natural phenomena are often considered complex systems including those with structure and dynamics that follow a power-law, systems at the critical point and/or systems exhibiting scale-free behavior or fractal properties due to a statistical self-similarity [1,2]. In this framework, particularly relevant is the study of fractal properties of electroencephalographic time series (EEG) [3] that have been largely investigated with various methods for diseases diagnosis as well as in order to point out the variation of complexity across different brain areas [4]. In this work we will focus on the free-scale and power-law properties of local neurodynamical signals as a measure of complexity. However, some systems have only seemingly scale-free behavior ending up in a skew probability distribution, that is log-normal instead of true power-law [5–7]. Moreover, some signals might exhibit a single power-law in the whole frequency domain, such as Brownian noise. In contrast, multifractal or multi-scaling time series exhibit heterogeneity and self-similarity only within some local ranges of the structure [8,9] and show a cascade of different power-law behaviors in different frequency ranges (meaning at different time scales) such as for example in cosmic rays [10], seismic activity [11] or tornadoes [12], heartbeat dynamics [13], fractal distribution of avalanches in neuronal recordings [14], and *1/f* noise associated with basic aspects of human cognition [15,16]. In general, fractality is not always evident, especially in environmental [17] or physiological time series, and the methods to measure it should be well assessed in order to avoid misleading claims [5,8,18]. The existence of different power-law regimes in the EEG spectrum is particularly challenging due to the overlap of well-known harmonics and broad band components [19]. However, the analyses of possible multi-scaling behavior of neurodynamics from intracranial electroencephalographic recordings with the purpose of looking for the differences across different brain areas are rather sparse and need further study.

The investigation of amplitude and frequency of typical oscillations in the power spectral density (PSD) of the neuronal signals was always around in the study of cognitive, behavioral and motor processes as well as in clinical research [20,21]. These spectrum-based methods primarily focus on periodic features and assume the stationarity of the signal over time (that means, that the unconditional joint probability distribution of signal does not change when shifted in time). On the contrary, the evaluation of the aperiodic activity is not always given special attention in the study of brain neurodynamics. This might be because the

* Corresponding author.
E-mail address: livio.conti@roma2.infn.it (L. Conti).

https://doi.org/10.1016/j.physd.2025.134733
Received 16 August 2024; Received in revised form 9 May 2025; Accepted 10 May 2025
Available online 10 May 2025

non-oscillatory components present in EEG signals, sometime called noise [22], is often referred to as an artifact or a result of an ensemble of narrow band overlapping periodic oscillations [23] or reconciled with some frequency band damped activity [24], and is many times removed or "averaged-out". However this aperiodic component can allow categorizing the non-specific and less predictable elements in the recorded brain signals possibly related to the cognitive or physiological processes [25]. Many structures, from various electronic devices [25,26] to the most complex systems, such as human brain neural activity, show to have aperiodic components, that can be seen as scale-free features and expressed as a power law behavior in frequency domain: $PSD(f) \sim 1/f^{\beta}$, with β exponent [22,27–29]. While some authors claim that *1/f* fluctuations in neural signals are noisy activity, other suggest that these non-oscillatory components are the uncorrelated noise that can enhance coherent dynamic brain activity [30], consolidate memories during sleep [31], acts as information transfer channel [32] can indicates the excitation and inhibition balance [33] or even show a possible relation between scale-free behavioral dynamics and scale-free cortex activity [16]. All of this supports the importance of studying such phenomena.

In order to estimate the scale-free or fractal features of the neural recordings a wide variety of fractality and complexity measures were adopted such as entropy [34], correlation dimension [35], detrended fluctuation analysis [36], Hurst exponent [37], normalized compression distance [38,39], Higuchi fractal dimension [40,41] and others [28,42,43]. However, these non-linear estimates might have different range of values in findings due to the algorithm dependences on various parameters, such as embedding dimension in the correlation dimension estimate [44], k_{max} value in the Higuchi's algorithm [45], and length of the window of the time series in the Hurst exponent or DFA [46,47]. This seems to be not only due to the intrinsic properties of the signals [47], the need of a better control of external/environmental variables and the limitations of possibly reduced datasets, but also to the need of a more rigorous mathematical approach of the adopted analysis tools [18].

In this work, we analyze intracranial stereotactic-electroencephalography (sEEG) recordings provided by the Montreal Neurological Institute (MNI) [48] from three gyri (superior temporal, postcentral and precentral), in physiological conditions, while subjects stay in resting wakefulness, REM, N2 and N3 sleep stages (Table S1). We analyzed the scaling properties of the PSD of the investigated areas looking for their distinguishing features. The aims of this study are: i) to verify if the difference of the mean PSD of sEEG recordings in certain frequency bands between cortical parcels and in a given wake/sleep stage allows distinguishing cortical areas; ii) to identify the power-law behavior of PSD across areas in wake/sleep stages and to measure the related β index; iii) to assess differences between the values of β exponent in high frequency range across cortical parcels in each single stage and across the four stages within a parcel.

2. Materials and methods

2.1. Datasets

The MNI dataset of intracranial stereotactic-EEG recordings, available at https://mni-open-ieegatlas.research.mcgill.ca/main.php, consists of recordings from 38 brain regions, of 1 min long each, and artifact free, detected at rest with closed eyes and in three sleep states (REM, N2 and N3) from 106 patients (13–68 years old, 48 females) investigated with cortical surface strip/grid electrodes [48]. Even though the subjects involved in the data acquisition were diagnosed with refractory focal epilepsy, the data provided by MNI was only from the regions not affected by the disease [48,49]. During the data taking period, medications have not been reduced [48]. The number of channels and subjects of dataset is non-homogenous in each area for wake and for sleep conditions due to the channel's exclusion criterion, that ensures the data analyzed in this study are only from regions not affected by epilepsy, and thus in physiological conditions.

Recently, Armonaite et al. [41,50], and other authors [4] by using the same MNI recordings, have shown how the measures of fractality, through the Higuchi procedure, can reveal the signature of cortical areas, however in a well selected population. Following them, here, we investigated the power-law properties of PSD for superior temporal gyrus (79 channels from 26 subjects), postcentral gyrus (64 channels from 21 subjects) and precentral gyrus (141 channels from 34 subjects) in wakefulness [49] (Fig. 1). The number of channels and subjects were reduced in the analysis during sleep, since, as mentioned, not all recordings were available in sleep stages [49].

2.2. Finding PSD characteristic harmonics

In order to analyze neurodynamical activity of the three investigated cortical parcels, we estimated the PSD (that is the squared spectral amplitude divided by the frequency) of each channel by applying a Fast Fourier Transform (FFT) with Hamming windowing, on sequences of 256 samples each (about 1.28 s long), that corresponds to a frequency resolution of ~0.78 Hz, with a sliding window no overlap. Due to the pre-processing low-pass filtering applied to the whole of MNI database in order to remove artefacts [48,49], the maximum frequency available is 80 Hz. For each channel, the PSD is normalized so that the area under each curve is equal to 1. We divided the frequency spectrum in the conventional 7 bands: delta (≤ 4 Hz), theta (4 – 8 Hz), alpha (8 – 12 Hz), low-beta (12 – 26 Hz), high-beta (26 – 33 Hz), low gamma (33 – 49 Hz) and high-gamma (49 – 80 Hz). We averaged the PSD of each channel within a subject and then across subjects for each cortical parcel, in order to obtain the normalized PSD within each band.

2.3. Fitting the PSD power-law exponent

On a double logarithmic scale, the PSD exhibits two approximately linear trends in the lower and higher portions of the spectrum, characterized by at least two (approximately) constant and different slopes (Fig. 2, right panel). Based on this observation and previous studies [22,27,51], we hypothesize that the neural activity contains different scaling regimes, and thus exhibit a cascade trend of different slopes. Since there are evidence that oscillatory activity can impact the slope of the PSD function on log-log scale, we first applied a low- (high-) pass Butterworth filter on each signal, (Fig. 2, left panel) with cut-off value of 4 Hz (33 Hz) for low (high) frequency range to eliminate the evident harmonic peaks. After, we estimated the PSD of each channel using 2048 FFT lines and then, for each *i*-frequency, we calculated the $PSD(f_i)$ average and the standard deviation (σ_i) across population, which is the global average across all channels and subjects. Since the variability between the subjects is higher than within-subject across channels, we adopted the most conservative approach and used the greater error, which is the global one across all channels and subjects. Then we calculated the linear fit by (separately in the low and high frequency range) by using the weighted least square method [52], where to each ordinate $y_i = \log(PSD(f_i))$ is associated the weight $w_i = 1/\Delta y_i^2$ with Δy_i the uncertainty on y_i. In the low frequency range, we excluded the first values of PSD (below about 0.29 Hz), which might be less reliable due to the residual contributions of delta and theta peaks, and evaluated the fit in 0.29 – 4 Hz range. Then, for the high frequency range, we estimated the power-law β exponent by fitting the mean PSD in the 34 – 80 Hz range. In order to assess the goodness of linear fit we evaluated the Pearson's r correlation test.

2.4. Evaluating the impact of tuneable parameters on fitting power-law exponent

The evaluation procedure of the linear fit of the PSD function includes some tunable parameters such as the spectral resolution, the low (high) cut-off frequency and the order of the filter. Thus, we selected various configurations of these parameters to find out how they impact

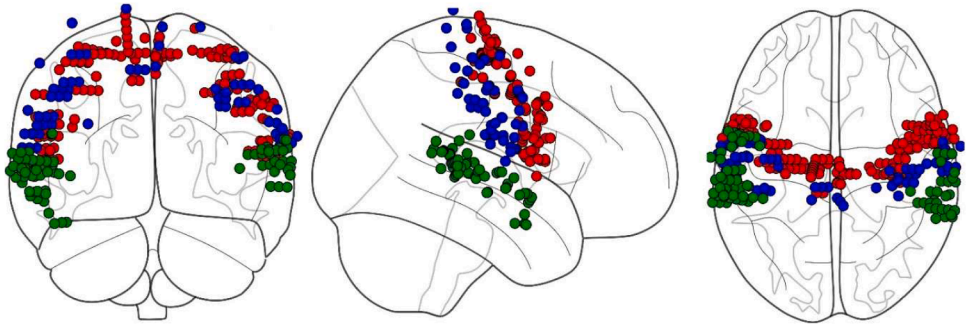

Fig. 1. The spatial distribution of the positions of all electrodes for sEEGs recordings in resting wakefulness available in the MNI dataset in the superior temporal gyrus (green, 79 channels), postcentral gyrus (blue, 64 channels) and precentral gyrus (red, 141 channels). Data comes from 55 subjects in total.

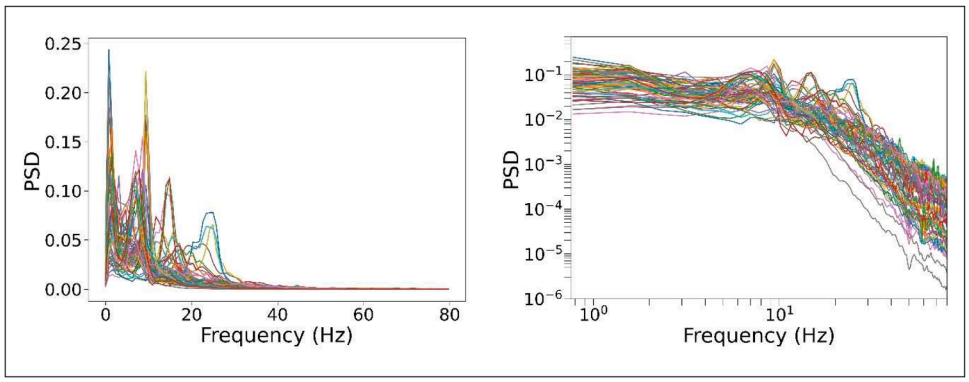

Fig. 2. The normalized PSD of all the 64 sEEG channels of the postcentral gyrus in wakefulness is given. In the left panel, several peaks in different frequency bands can be observed. In the right panel, the same plot is given on a double-logarithmic scale: two linear trends (suggesting multiple power-law behaviors) can be observed in the lower (below few fractions of Hertz) and higher (for f $\gtrsim$ 30 Hz) frequency ranges. A qualitatively similar trend of PSD (including peaks and power-law behavior) is observed in the sEEG channels for the precentral and superior temporal gyri of MNI data.

the final result. For the low- (high-) frequency range, we tested cut-off value of 4 Hz and 8 Hz (33 Hz and 50 Hz) for the low- (high-) pass Butterworth filter. In both cases we tested the filter order $n = 5$ and $n = 7$, together with various frequency resolution values by changing the length of the FFT window (between 256, 1024 and 2048 samples). The results of fitting with various combination of tunable parameters are

Table 1
Here we provide the post-hoc Tukey-HSD test Q_{test}, that is the difference of the mean band PSD between couple of areas (postcentral (PostG), precentral (PreG) and superior temporal (STG) gyri), separately in seven frequency bands and for each wake/sleep stage. The Q_{test} and p values are bolded if $p \leq 0.05$. Values are *italicized* if one cortical parcel has greater PSD than the other two. Q_{test} is positive (negative) according with the sign of the difference between the mean band PSD of two compared areas. Zero p means value lower than 0.001.

			δ	θ	α	lβ	hβ	lγ	hγ
Wake	PreG-PostG	Q_{test}	**−0.0094**	−0.0019	**−0.0118**	***0.0053***	***0.0022***	***0.0005***	0.0001
		p	**0.018**	0.856	**0.000**	***0.001***	***0.003***	***0.024***	0.504
	STG-PostG	Q_{test}	***0.0183***	0.0005	0.0003	**−0.0043**	**−0.0023**	**−0.0005**	−0.0001
		p	***0.000***	0.993	0.994	**0.024**	**0.005**	**0.023**	0.229
	STG-PreG	Q_{test}	***0.0277***	0.0024	**0.0121**	***−0.0096***	***−0.0044***	***−0.0010***	**−0.0002**
		p	***0.000***	0.759	**0.000**	***0.000***	***0.000***	***0.000***	**0.005**
REM	PreG-PostG	Q_{test}	−0.0073	−0.0042	−0.0006	***0.0024***	***0.0019***	0.0003	0.0000
		p	0.313	0.226	0.954	***0.019***	***0.008***	0.206	0.917
	STG-PostG	Q_{test}	***0.0130***	**−0.0099**	−0.0003	−0.0005	−0.0006	−0.0003	−0.0001
		p	***0.044***	**0.001**	0.992	0.842	0.665	0.221	0.146
	STG-PreG	Q_{test}	***0.0203***	**−0.0058**	0.0003	***−0.0030***	***−0.0025***	**−0.0006**	**−0.0001**
		p	***0.000***	**0.027**	0.981	***0.001***	***0.000***	**0.000**	**0.017**
N2	PreG-PostG	Q_{test}	**−0.0186**	0.0031	**0.0089**	***0.0025***	***0.0005***	0.0001	0.0000
		p	**0.000**	0.402	**0.000**	***0.000***	***0.005***	0.058	0.445
	STG-PostG	Q_{test}	−0.0071	**0.0060**	0.0049	−0.0005	−0.0002	−0.0001	0.0000
		p	0.305	**0.050**	0.096	0.710	0.521	0.585	0.983
	STG-PreG	Q_{test}	**0.0115**	0.0029	−0.0040	***−0.0030***	***−0.0007***	**−0.0002**	0.0000
		p	**0.010**	0.344	0.092	***0.000***	***0.000***	**0.000**	0.237
N3	PreG-PostG	Q_{test}	**−0.0181**	**0.0065**	***0.0090***	***0.0016***	0.0002	***0.0001***	**0.0000**
		p	**0.000**	**0.012**	***0.000***	***0.003***	0.148	***0.015***	**0.045**
	STG-PostG	Q_{test}	−0.0054	**0.0061**	0.0015	−0.0003	−0.0001	0.0000	0.0000
		p	0.432	**0.030**	0.753	0.817	0.638	0.999	0.739
	STG-PreG	Q_{test}	**0.0127**	0.0004	***−0.0075***	***−0.0019***	**−0.0003**	***−0.0001***	0.0000
		p	**0.001**	0.980	***0.000***	***0.000***	**0.003**	***0.003***	0.145

provided in Table S2 and Table S4 for low and high frequency range respectively.

2.5. Investigating independence of power-law exponent from subject features

The population in the dataset was highly variable with respect to age. Thus, we also evaluated if the β slope could vary with respect to age and to sex. We performed the estimate of Pearson's correlation only for the high frequency range, since a more reliable linear tendency is visible in this range.

2.6. Statistics

For every channel, after having computed the normalized PSD, we calculated its mean value in each of the seven conventional frequency bands. We investigated the differences of the mean band PSD between the cortical parcels in wake, REM, N2 and N3 sleep stages separately. To assess the statistical significance of the differences between parcels in each band, we used the post-hoc Tukey-HSD test [53] of the analysis of variance (ANOVA). We deployed the test on the group of interest; the three cortical parcels in each band and each state. We provide the differences between the two parcels as a Q_{test} and a corrected p-value with a scaler equal to 3 (Table 1).

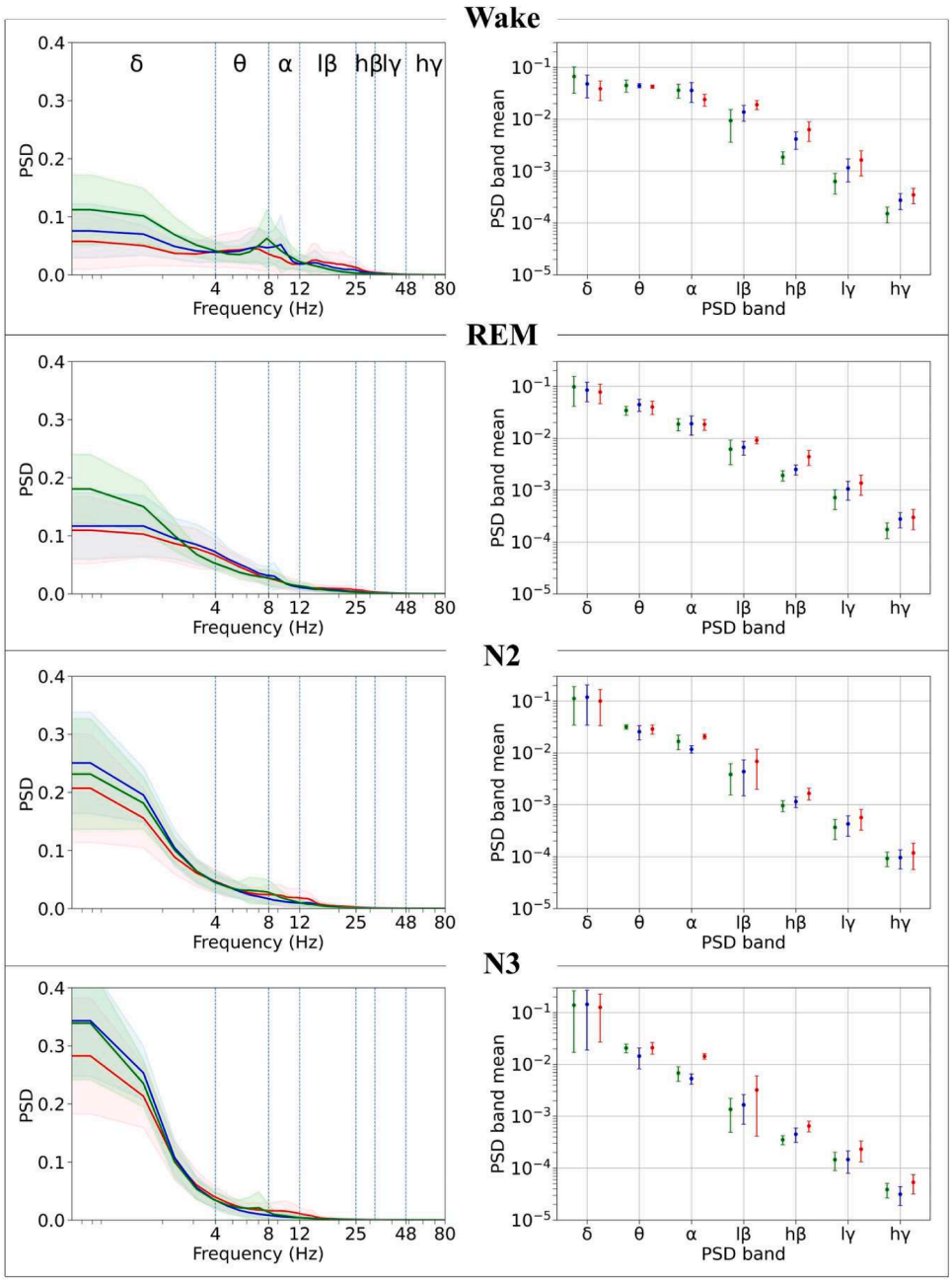

Fig. 3. The normalized PSD (averaged across all sEEG channels) compared between the superior temporal (green), postcentral (blue) and precentral (red) gyri is shown in the panels (from top to bottom) for wakefulness, REM, N2 and N3 sleep stages respectively. On the left column, the PSD in each area with the standard deviation (represented by the colour filled region) is plot vs frequency. The y-scale is cut at the amplitude equal to 0.4 in order to avoid a compression of the graphs. On the right column, we provide the PSD mean and standard deviation evaluated in each of the 7 frequency bands investigated. The statistical results, about the significance of the differences between the PSD in the three parcels compared in each band, are given in the Table 1.

For the power-law β exponent - estimated in low- and high-frequency ranges from the fit of the PSD averaged on all channels, in each wake/sleep state separately - we carried out a similar comparative analysis between the pairs of cortical parcels and across states by deploying a *T*-test. The test was carried out on each couple of regions given the mean, standard deviation and number of observations in the two compared groups (see Table 3). In low frequency range, the study was carried out only in wakefulness.

3. Results

3.1. Band PSD across areas during wakefulness and sleep

We investigated whether, in a specific frequency band, the mean PSD of sEEG measured in one of the three investigated cortical parcel is significantly higher/lower than in the other two, indicating a spectral signature of a cortical area. After having performed the post-hoc Tukey-HSD test, we observed that the PSD of superior temporal gyrus is the highest in delta frequency band ($p \leq 0.05$), instead precentral gyrus prevails in low beta ($p \leq 0.01$) band, both in wakefulness and REM sleep. Postcentral gyrus shows more prominent activity than precentral gyrus ($p \leq 0.01$), but not significantly more than superior temporal gyrus, in alpha band, only in wakefulness. We also observed that precentral gyrus expressed higher activity than the other two gyri in high beta and low gamma frequency bands ($p \leq 0.02$) in wakefulness. An evident transit from higher frequencies to the lower ones is seen in N2 and N3 sleep stages in precentral gyrus, where the prevalent frequencies are low beta in N2 stage and alpha as well as low beta in N3 sleep stage ($p \leq 0.01$). In the other two regions, the PSD peaks are more ubiquitous and indistinguishable in about all frequencies. The results are depicted in Fig. 3 and Tukey-HSD statistics (Q_{test}) with associated p values are summarized in Table 1.

3.2. Power-law β exponent across areas in wakefulness

We looked for power-law behavior in PSD of sEEG recordings in wakefulness in the lower frequency range (below about 4 Hz, mainly in delta band) and in the higher frequency range (above about 30 Hz, mainly in high-beta and gamma bands). In low frequency range, the steepest slope is observed in superior temporal gyrus followed by postcentral and precentral gyri. However, the linear fit indicated by Pearson's correlation $|r| < 0.9$ is not optimal, being probably still affected by residual contributions of delta and theta peaks, and consequently the estimation of β suffers of a larger uncertainty. In fact, the statistical errors on the β values for different parcels in low frequency range overlap and do not allow to distinguish the parcels in this frequency range Therefore here we focus only on results for the high frequency range. However, for the sake of completeness, we provide also the results of fitting in the low-frequency range in the supplementary materials (Table S2, Table S3 and Fig. S1, Fig. S2). Instead in the range between 33 and 80 Hz, for all combination of the tunable parameters, the fitting showed almost perfect linearity with $|r| > 0.9$ (Table S4). In the Fig. 4A, we show the linear fit in the high frequency range for the three cortical parcels for wakefulness. We found statistically significant differences between the three areas ($p < 0.001$), with an inverted order with respect to the lower frequency range fitting value β, where the steepest slope, thus highest β value, was observed in precentral gyrus, following postcentral gyrus and then superior temporal gyrus (Fig. 4B and Table 2). In both frequency ranges, we have verified that changing the specific values of tunable parameters the linearity of the spectrum - that is the power-law behavior - is quite stable and the estimated value of β does not change significantly within the errors of measurement (Fig. S3).

3.3. Scale-free activity during sleep

Having assessed the β values in wakefulness we performed the same analysis during sleep stages. In low frequency range, during REM, N2 and N3 sleep stages the estimation of β is less reliable than during wakefulness as shown in the case of N2 in Fig S4). One of the reasons might be that during sleep stages, the amplitude of delta PSD peak is particularly high, and thus overwhelms the scale-free behavior in the low frequency range (Fig. S4). Instead, in the high frequency range (such as high-beta and gamma bands), the linearity of the PSD behavior is evident also during all sleep stages (Fig. 5A.). Moreover, we found that in this frequency range the β values in sleep stages are statistically different across parcels (Table 3A.) and have the same relationship

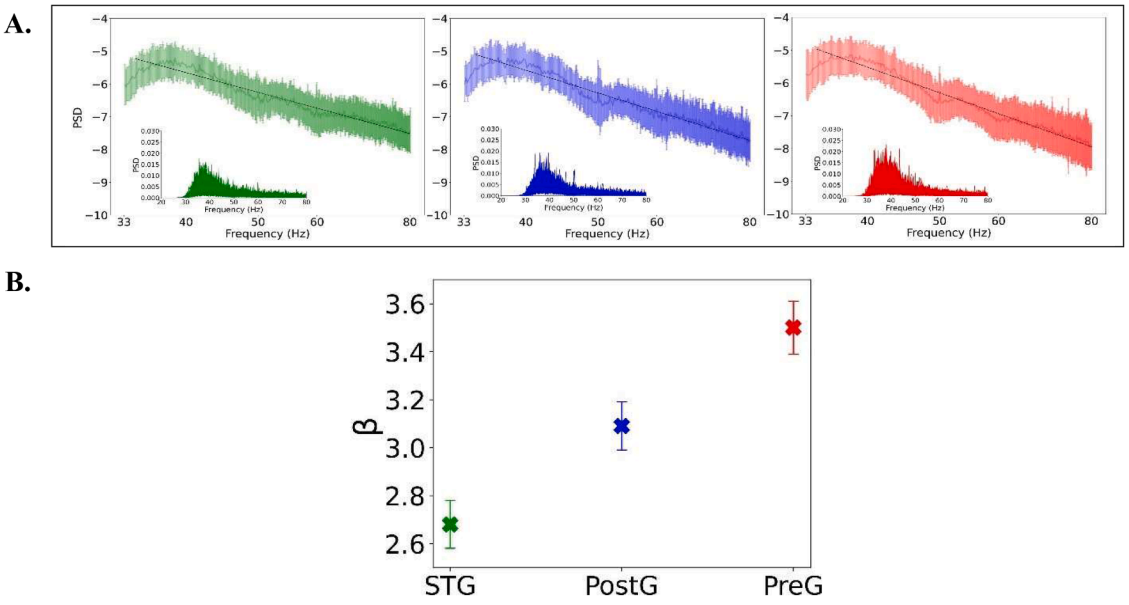

Fig. 4. A. Estimation of the power-law exponent β of PSD on a double logarithmic scale for wakefulness in the three gyri: superior temporal (green), postcentral (blue), and precentral (red). The inset figures represent each signals PSD after having used Butterworth filter of order 7 with cut-off at 33 Hz, 2048 FFT lines and in range 33 - 80 Hz. B. Comparison of the value of the power-law β exponents (evaluated in wakefulness in the high (34 – 80 Hz) frequency range) between the three gyri (STG - superior temporal in green, PostG - postcentral in blue and PreG - precentral in red). The values of β with the estimated error are summarized in Table 2.

Table 2
Comparison of slope (β) and intercept values of the linear fit of PSD, across parcels and in four wake/sleep states for the high-frequency range having used Butterworth filter of order 7, with cut-off at 33 Hz, and 2048 FFT lines.

	Wake		REM		N2		N3	
	β	Intercept	β	Intercept	β	Intercept	β	Intercept
STG	2.68 ± 0.10	4.24 ± 0.40	2.71 ± 0.09	4.38 ± 0.38	2.71 ± 0.09	4.38 ± 0.36	2.65 ± 0.09	4.13 ± 0.36
PostG	3.09 ± 0.10	5.82 ± 0.41	2.96 ± 0.09	5.34 ± 0.38	3.01 ± 0.09	5.52 ± 0.37	2.84 ± 0.09	4.86 ± 0.37
PreG	3.50 ± 0.11	7.40 ± 0.45	3.10 ± 0.10	5.87 ± 0.40	3.28 ± 0.10	6.57 ± 0.39	3.05 ± 0.09	5.67 ± 0.38

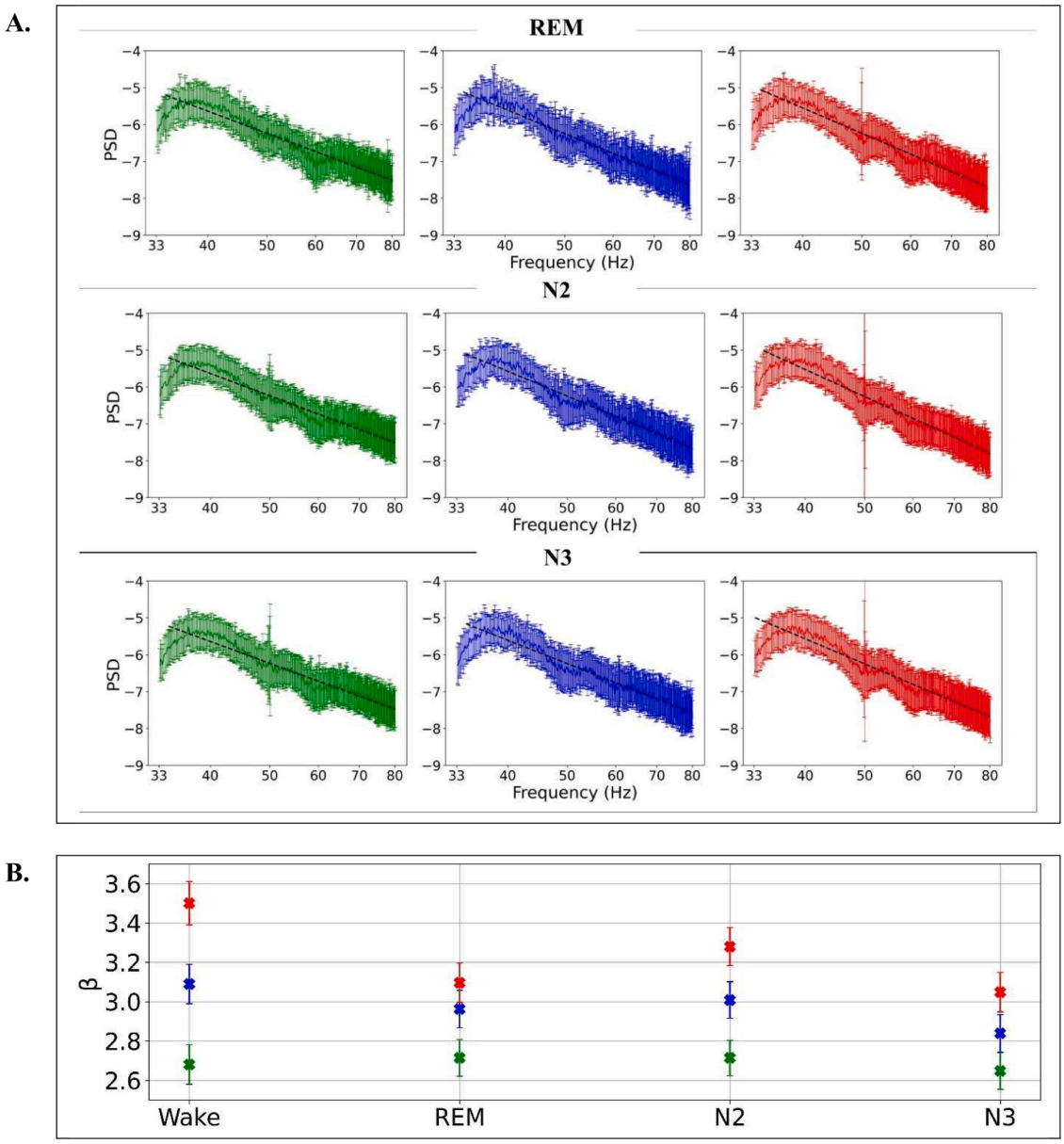

Fig. 5. A. Estimation of the power-law β exponent β of PSD in sleep. We present the linear fit of the mean PSD vs frequency in a log-log scale, in the high frequency range, for superior temporal (left panel), postcentral (central panel) and precentral (right panel) gyrus during REM, N2 and N3 sleep stages. B. The β values of the PSD fit in the frequency range 34 - 80 Hz are compared across the three gyri (superior temporal (green), postcentral (blue) and precentral (red)) separately in the wake/sleep stages. In each stage, the difference between β values allows distinguishing the investigated regions beyond the error bars. Moreover, in each stage the relation between the β values of the three areas shows stably that $\beta_{STG} < \beta_{PostG} < \beta_{PreG}$.

between the areas pointed out in wakefulness: precentral gyrus has higher β value than postcentral gyrus and both higher than superior temporal gyrus (Fig. 5B and Table 2). This is one of the main results of our analysis: the β value estimated in the high frequency range might indicate the possibility to distinguish the areas, beyond the fitting error, in each wake/sleep stage.

Then we investigated how in each fixed cortical parcel, the β value changes from wakefulness across sleep stages. It is notable that, while β value varies between the regions within each fixed state, it stays rather stable across states in each single region (Fig. 5B and Table 3B). On the

Table 3
Statistical *T*-test (T_{test}) for the comparison of the β values evaluated in high frequency range, between couple of regions in each of the four wake/sleep states (panel **A.**) and vice versa between pairs of states in each region (panel **B.**). We use abbreviations PostG, PreG and STG for postcentral, precentral and superior temporal gyri respectively. T_{test} is positive (negative) when the β value of the first region is higher (lower) than that of the second one. Zero p means value lower than 0.001. The areas are distinguishable between them in each wake/sleep state.

A.		Wake	REM	N2	N3
PostG-PreG	T_{test}	26.35	6.98	15.76	12.70
	p	0.00	0.00	0.00	0.00
PostG-STG	T_{test}	24.38	11.95	17.16	10.87
	p	0.00	0.00	0.00	0.00
PreG-STG	T_{test}	56.27	21.91	38.20	28.10
	p	0.00	0.00	0.00	0.00

B.		PreG	PostG	STG
Wake-REM	T_{test}	26.57	6.36	−1.72
	p	0.00	0.00	0.09
Wake-N2	T_{test}	15.92	4.31	−1.92
	p	0.00	0.00	0.06
Wake-N3	T_{test}	34.40	13.47	1.92
	p	0.00	0.00	0.06
REM-N2	T_{test}	−11.47	−2.36	0.00
	p	0.00	0.02	1.00
REM-N3	T_{test}	3.33	5.66	3.50
	p	0.00	0.00	0.00
N2-N3	T_{test}	16.66	8.76	3.92
	p	0.00	0.00	0.00

other hand, it seems that there is a reduction of the dispersion of the β values between the three areas, from wake (largest spread) up to N3 (minimum spread). This reduction is questionable because it would be essentially driven by the β value of precentral gyrus in wake (one value of β over the twelve measured in 4 states of 3 areas). Analyzing separately the areas, we observed that the β values are almost independent from the wake/sleep stage in postcentral gyrus ($p = 0.02$) and about constant ($p = 0.07$) in superior temporal gyrus. On the contrary a variability of β across wakefulness and three sleep states is visible ($p < 10^{-6}$) in precentral gyrus, which corresponds to a primary motor cortex; this might happen due to micro movements during resting wakefulness and movement related potentials involvement during sleep [54]. Moreover, in N2 the β of precentral gyrus is higher than in REM, that could not confirm the "smooth" reduction of power-law exponent from wake to deep sleep (N3) suggested by some authors [19].

In order to further investigate this point, in Fig. 6, we analyzed the variation of β values versus the PSD mean in delta band ($<PSD>_\delta$), that is a good indicator of wakefulness activity and the depth of sleep [55]. We also tested the hypothesis of a linear dependence of β from $<PSD>_\delta$

Table 4
Test of the hypotheses of constancy or linear dependence of β exponent from the wake/sleep stage, in a fixed cortical area. We show the ANOVA F_{test} between the estimations of β in the 4 wake/sleep stages and the results of the linear regression ($\beta = \beta_0 + \lambda <PSD>_\delta$). The β values seem independent from wake/sleep stages in superior temporal gyrus and barely dependent in postcentral gyrus, while in precentral gyrus both the hypotheses of constancy and linearity are rejected. The eventual stability of the β value in some regions, across wake/sleep stages, could imply that the scale-free activity component that we are pointing out is about independent from the wake/sleep conditions or at least not significantly affected by them.

	Hypothesis of constancy		Hypothesis of linear dependence			
	F_{test}	p-value	β_0	λ	r	p-value
STG	6.1	0.07	2.74 ± 0.20	−0.45 ± 1.83	−0.36	0.64
PostG	61.2	0.02	3.19 ± 0.14	−2.15 ± 1.33	−0.85	0.15
PreG	291.4	$< 10^{-6}$	3.60 ± 0.15	−4.29 ± 1.61	−0.80	0.20

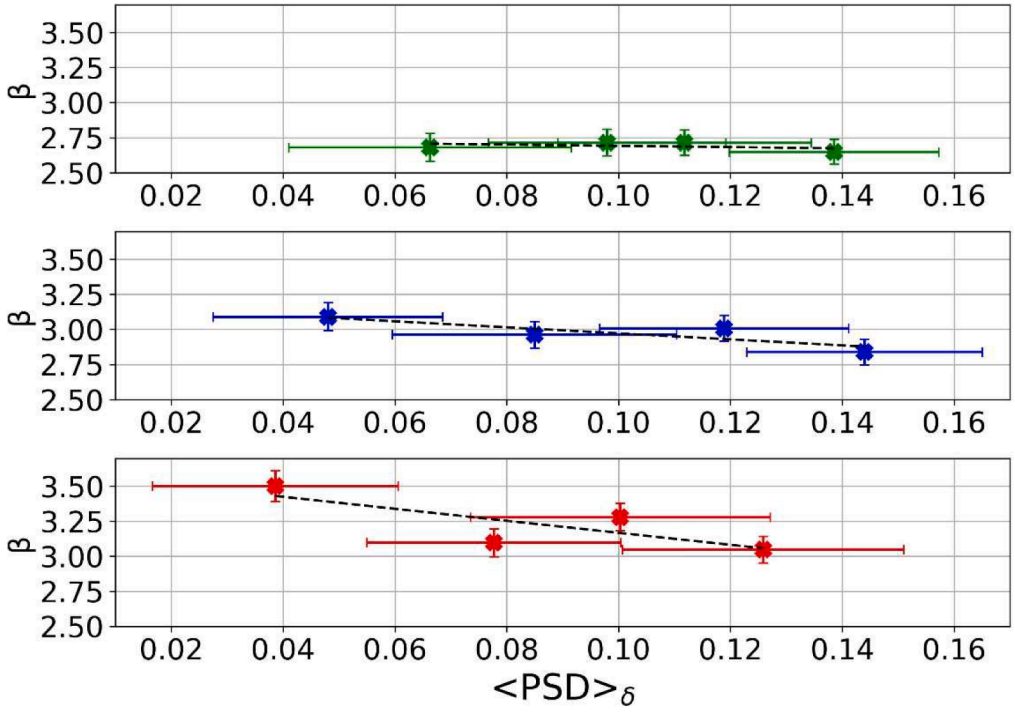

Fig. 6. Comparisons of β values across wake/sleep states, in each cortical region. The β values of the PSD's fit in the high frequency range, for the three gyri (superior temporal (top panel, green); postcentral (central panel, blue) and precentral (panel, red)), are presented as a function of the mean of PSD amplitude in delta band $<PSD>_\delta$. In general, we observe a large variability of mean PSD in delta, expressed by the horizonal error bars. In superior temporal gyrus (bottom panel), the β values in the all wake/sleep stages are indistinguishable between them within the vertical error bars. In postcentral gyrus (central panel), only β values in "farthest" conditions - that is with lowest/highest PSD in delta (corresponding to wake and N3 respectively) - are distinguishable beyond the vertical errors. Finally, in precentral gyrus (top panel), the β value in wake is different from values in REM, N2 and N3, that instead are not (or not completely) distinguishable between them.

(Table 4) obtaining that it can be excluded in all parcels. Even though further analyses are needed, the stability of the β value in two regions, across wake/sleep stages - together with the "instability" in the pre-central gyrus - could imply that in these two cases the component of the scale-free activity, that our procedure is pointing out, is about independent from the wake/sleep conditions or at least not significantly affected by them, while the apparent "instability" in motor cortex could be compatible with the reduction reported in literature.

In order to represent the spatial distribution of scale-free activity across the areas, in Fig. 7 we provide a map of β, suitably normalized over brain parcels and sleep stages, in several brain projections. We focus only on β calculated in higher frequency range. The investigated areas are colored on the basis of the ratio $\Delta\beta_{ij}$ defined as:

$$\Delta\beta_{ij} = \frac{(\beta_{ij} - \beta_{min})}{(\beta_{max} - \beta_{min})} \tag{1}$$

where β_{ij} indicates the power-law exponent in the *i*-area (i = superior temporal, postcentral and precentral gyrus) and *j*-state (j = wake, REM, N2, N3). In panel A of Fig. 7, β_{min} (β_{max}) stands for the relative minimum (maximum) value of β computed over the three areas, separately for each wake/sleep stage. Instead in panel B of Fig. 7 we use the absolute minimum (maximum) of β evaluated over the three areas and the four states all together. In both cases, the $\Delta\beta_{ij}$ value ranges between 0 and 1. The graphic representation of panel A confirms that the map (i.e., the color contrast) of the investigated areas is stable in the different stages, i.e., β is reliable in distinguishing them; while panel B shows that with the normalization of $\Delta\beta_{ij}$ over all stages and areas the ability to distinguish (resolve) areas slightly improved in wakefulness and N2.

3.4. Independence of power-law exponent from age and sex

Since the population analyzed in this work come from different age groups, we verified if the β value estimated in high frequency range for each investigated cortical parcel correlate with age. By evaluating the Pearson's test on the ensemble of β vs age, we obtain ($r = 0.37, p = 0.86$) for superior temporal gyrus; ($r = -0.09, p = 0.71$) for postcentral gyrus and (r = - 0.09, p = 0.63) for precentral gyrus. Therefore, we can conclude that not statistically significant correlations are found between β and age in each of the three parcels mentioned. We have also investigated the existence of a possible dependence of β exponent from sex: by separating population in male and female groups we do not observe any statically significant cluster separation with respect to β value.

4. Discussion

4.1. Spectral and fractal features of local neurodynamics

It is known that brain is organized in hierarchical structures so that the smaller units, that serve specific functions, interact within the broader context of large-scale networks, connecting distant regions throughout the brain [56]. While the whole brain regions clustering from resting state functional imaging is rather well assessed [57], looking for the features from the instantaneous neural recordings in different brain parcels is also emerging [58]. Keitel and Gross [59], using the magnetoencephalographic (MEG) recordings from healthy subjects, clustered the PSD functions, and found significant spectral features characteristics of different cortical parcels. Alpha components prevail in anterior brain regions, delta in the temporal region, whereas beta and gamma in more posterior region. Furthermore, Frausher et al., [48], by analyzing the neurodynamics from intracranial EEG recordings, found characteristic oscillations, such as the alpha rhythms in the occipital lobe, parietal lobe and temporal lobes; lower beta in the postcentral gyrus; higher beta and gamma oscillations in precentral gyrus. Further research of features of the neural activity in the different brain parcels was performed with fractal measures. Primary motor and primary somatosensory cortices were evaluated from the scalp EEG, where the higher fractality was observed in primary motor cortex within each subject [60]. Thus, our findings are in line with previous studies.

4.2. Oscillatory versus non-oscillatory neural activity

The PSD of each of the sEEG channels in the three investigated gyri shows relevant peaks at certain typical frequencies,(such as mainly in the delta, theta, alfa and beta bands) (Fig. 2, left panel) and a linear trend of PSD vs frequency in a log-log scale mainly in gamma band (Fig. 2, right panel). However, there are claims, that the PSD slope in a double – logarithmic scale would not represent a power-law behavior but is a mere effect of the damped periodic oscillations of neural activity [24]. In Fig. S5 we show an example of such mechanism. It has been also shown that high PSD peak in alpha band correlates with high power law exponent measured at higher frequencies [61]. On the other hand, He et al. [22] arguments that rhythmic, recurring patterns of brain activity in a certain range of frequencies, and arrhythmic activity (with no prevailing frequency) are distinct and the latter indicates scale-free dynamics. The same authors also pointed out that, however, periodic oscillations (such as those prevailing in 8 – 12 Hz frequencies in resting state) can generate "hills" in the log-log scale representation of the power spectral density versus frequency, that will artificially surge the slope β at higher frequencies. Therefore, in order to verify the existence of power-law behavior of PSD and estimate its β index, it is necessary to pre-process data in order to eliminate the periodic components.

Several methods have been proposed in literature to assess the scale-free activity of neurophysiological recordings. One of them is the detrended fluctuation analysis (DFA) [62], in which the time series is subdivided into m equal length sub-sets, where in each the signal is approximated with a fixed-order polynomial. Then the fluctuation around the trend is computed through the root mean square evaluated for each segment and eventually averaged for different m sub-set lengths, which means considering different scales. Another adopted method requires to identify the low-frequency components of PSD and to remove them before computing a detrended time series by the inverse Fourier transform [63]. Not to mention the widely used coarse graining spectral analysis (CGSA) [64] based on similar technique as DFA. Finally, a recently suggested technique to extract scale-free features is the parametrizing of the power spectrum into periodic and non-periodic oscillations [29].

Most of mentioned procedures are based on the resampling or a polynomial approximation of whole or portions of the signal. In this work, instead we removed the oscillations in sEEG signals below (above) a certain frequency threshold ω_c by applying a Butterworth filter of order n with transfer function H:

$$|H(n, j\omega)| = \frac{1}{\sqrt{1 + \left(\frac{\omega}{\omega_c}\right)^{\pm 2n}}} \tag{2}$$

where the ± sign refers to the low/high pass filter that flattens the spectral content above/below the cut-off value ω_c. The sharpness of the filter depends on its order. The filtering procedure is well assessed in literature, with few parameters (only the filter's order and cut-off frequency) and is robust, being independent from the specificity of the signals. Therefore, we consider that our approach is preferable being the most conservative one. Moreover, differently from the others techniques, the filtering procedure allows to regulate the frequency threshold up to or from which we are seeking to remove the oscillations.

4.3. Different scaling trends in neurophysiological time series

In a previous study [65], authors found that β estimated in the frequency range 3 - 100 Hz in wakefulness and sleep was 2.02 ± 0.30 and 3.19 ± 0.31 respectively. Another study, performed in different

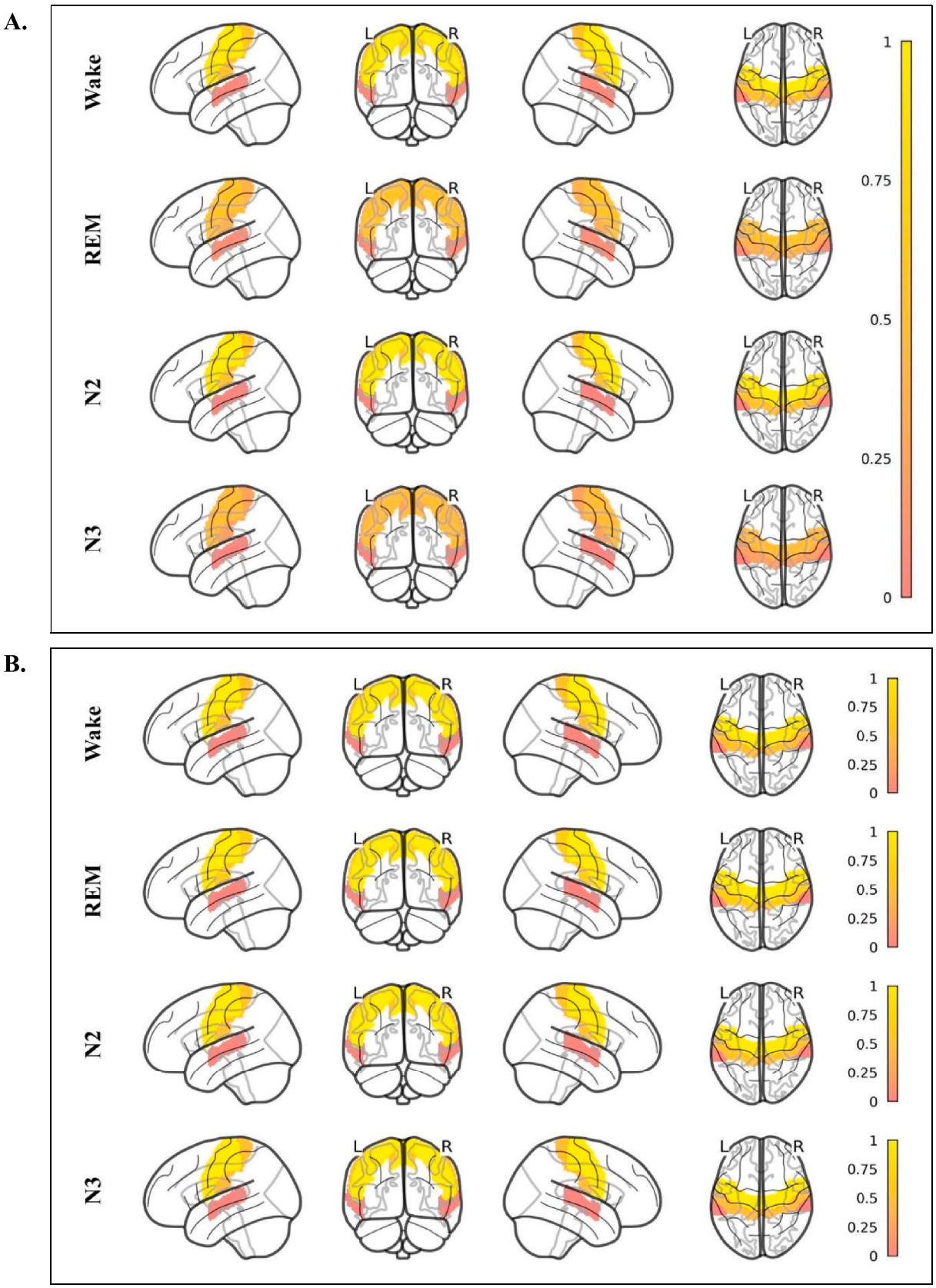

Fig. 7. Map of the brain in four spatial projections, shown from top to bottom for wakefulness, REM, N2, N3 states, for β calculated by fitting PSD in high frequency range. The investigated areas are coloured on the basis of the value of ratio $\Delta\beta_{ij}$ of the power-law exponent. See text for details. In panel **A** the $\Delta\beta_{ij}$ ratio is normalized only over the three areas, while in panel **B** the ratio is normalized over both the areas and the wake/sleep states. In both cases, the $\Delta\beta_{ij}$ values range between 0 and 1.

frequency ranges, found that $\beta \geq 4$ above 80 Hz; whereas below 80 Hz $\beta \approx 2.5$ [66].

Several previous studies have evaluated the different scaling regions in the neurophysiological recordings. Miller et al. [66] analysed power-law scaling in subdural electrocorticographic recordings from the surface of human cortex and observed a "knee" in the PSD at about 75 Hz, which would indicate a characteristic different time scales. The analysis was performed in two frequency ranges; where they found power-law exponent $\beta = 4$ above 80 Hz; whereas below 80 Hz $\beta \approx 2.5$. Importantly, they observe that this index remains stable across subjects.

He et al. [27] also investigated the behavior of PSD vs frequency of the electrocorticogram (ECoG) in wakefulness. As in the mentioned study, also these Authors found a "shoulder" behavior in the spectrum which they associate with the oscillatory activity. To eliminate the harmonic contributions, authors used a CGSA procedure. They fit separately the lower (< 0.1 Hz) and the higher frequency range (1–100 Hz). For the lower frequency range, they found that the value of the β exponent were: 2.2 and 1.60 in wakefulness and sleep respectively. These results are not compatible with our findings in low frequency range, but this might be because of rather different frequency range and other parameters for fitting procedure. On the other hand, the large variability of the estimations of PSD slope in low frequency range is also supported by the results of the investigation in patients with migraine via fMRI scan, that indicated that the value of the power-law exponent calculated at ultralow frequency range (up to 1 Hz) can vary from 0.5 to 1 [67]. These results are compatible with our findings in low frequency range. Even though, the low frequency range fit is generally less reliable, we still observe that the slope is not zero (as would be in the case of pure Gaussian noise). That supports the hypothesis that also the investigated low frequency range could show some scale-free properties in agreement with the literature, that is in partial numerical agreement with published reports obtained in similar measurement conditions [22,27,28]. In the higher frequency range, the PSD shows a more stable power-law behavior, as in the study that He et al. [27] has conducted obtaining β to be 2.44 and 2.87 respectively in wakefulness and slow wave sleep. At high frequencies, our results of β are comparable with this and other studies, where, in general, β is found to be in the range $2 \leq \beta \leq 4$.

Instead, Frauscher et al. [48] have also evaluated the non-linear component of the sEEG time series in different brain regions. They applied a CGSA pre-processing technique, and estimated β in the 10 - 40 Hz frequency range. They haven't found significant differences of β across all lobes, but only among fusiform and para-hippocampal gyri, middle frontal gyrus as well as inferior occipital gyrus and occipital pole.

The scaling properties has also been studied from the scalp EEG, with the scope to investigate the changes in the schizophrenia [68], where authors found that the slope of the PSD in schizophrenic patients was significantly steeper compared to controls. Similar study was conducted in Alzheimer's disease, where authors find significantly decreased β slope in Alzheimer's disease for every EEG scalp electrode [69].

All of this shows the importance of the scale-free neural activity, but also the debate about the existence of power-law behavior, the estimation procedure, the variability of computed β exponent and the multiple-power law components, and that proper measures to look for non-oscillatory brain electrical activity are yet to find. Despite that, our results suggest that in the neurophysiological time series there might be a scale-free activity component that might differ from one cortical parcel to another (such as a feature allowing to distinguish them) and is possibly stable to the change of the wake/sleep state. This supports our hypothesis that power-law exponent can constitute a suitable parameter for cortical parceling.

4.4. Possible origin of the scale-free activity and the scaling stability across wake/sleep stages

The origin of the scale-free activity is highly debated. There are claims that the scale-free and fractal nature of brain dynamics and power-law behavior could occur merely due to the superposition of random components acting on multiple time scales [70] or that the power-law is an artefact due to many averaged narrow-band periodic oscillations of different amplitudes and frequencies [71]. Other authors proposed that the power-law behavior would be due to the rapid exponential rise and slow exponential decay of dendritic response to an impulse input convolved with Poissonian process pulses [65]. Evertz, Hicks, and Liley [24] in a recent paper suggested a model that the power-law property originates from the overlap of several independent damped oscillations in alpha band that would modulate the power spectrum in that band.

Another source of scale-free fluctuations could be self-organizing phenomena. Self-organizing criticality implies that neural networks naturally arrange themselves to a state where small events, like a single neuron firing, can lead to large-scale cascades of activity [72]. This state is believed to optimize information processing, allowing the brain to efficiently respond to stimuli and adapt to changing conditions. The criticality in neural activity refers to the balance between stability and flexibility that enables the brain to respond rapidly to new information while maintaining some level of stability [51]. This idea can indicate that neural cell holds, as a general property, the ability to adapt being at the critical point. Thus, without external stimuli, this property might remain stable that could explain the stability of the power-law exponent across wake/sleep stages.

Another hypothesis suggests that $1/f$ fluctuations may stem from the biophysical properties of cells and the extracellular filtering property, due to the complex arrangement of electrical impedance of the inhomogeneous extracellular media [73]. In the absence of stimuli, the properties of the cellular media might remain unchanged. Furthermore, the scale-free component in the brain may connect temporal scales in the dynamics of neural activity, rather than be expressed as an amplitude, as seen in oscillatory activity. This might explain why spectral exponents in wake/sleep states remain unaltered, as scale-free fluctuations appear to be independent of amplitude [74]. It's noteworthy that Bedard, Kröger, and Destexhe [74] also observed a stable scale free effect in the higher spectrum range during wakefulness and slow wave sleep.

5. Conclusion

Our results suggest that at high frequency the local neurodynamics of different cortical parcels might hold different scale-free signatures despite the state. However, we still do not have complete control of the various factors that may impact the manifestation of the power-law behavior and the estimation of its exponent, especially in the low frequency range, possibly due to the overlap with high delta oscillatory activity [74]. Also, the fitting range has a further necessity for investigation, as it might slightly impact the β value. Furthermore, there is a need to evaluate and compare various methods to detrend the periodic oscillations before estimating the power-law exponent, as the technique for deletion of the oscillatory activity could also affects the linearity and thus the β value. The analysis presented could also be applied to further brain areas investigated from both intracranial and scalp EEG recordings. Such study is particularly relevant for the future studies of local neurodynamics from the scalp EEG/MEG, because there are possibilities to separate the source of the signal with methods such as Functional Source Separation (FSS) [75], and therefore analyze the fractal neurodynamics activity in a specific cortical area from outside the scalp. Such study could give incentives for classification of cortical areas according to the local ongoing neuronal activity.

Glossary

Neurodynamics – resting state spontaneous ongoing electrical activity of the neural networks sets.

Intracranial stereotactic electroencephalography – neuronal activity recordings directly from the cortex and subcortical areas

registered with electrode grids and strips.

Oscillatory neural activity – the periodic component of the neuronal electrical activity detected from the scalp or intracranial electroencephalographical recordings with typical peaks between 8 and 12 Hz, in healthy subjects, resting state wakefulness.

Coarse graining spectral analysis – a signal processing technique based on spectral signal analysis in order to point out the relationships between different signals.

Power law of power spectral density – the linear dependence of the logarithm of the power spectral density as a function of the logarithm of frequency, where the power spectral density decreases as the frequency increases showing the property of scale invariance.

Scale – free (scale invariance) – the property of a system whose behaviour remains unchanged regardless of the time scale or the scale of other variables. This also implies a self-similar or fractal structure.

Fractal – a complex geometric shape that at different scales maintains an exact or similar structure and often have non integer dimension.

Abbreviations

PSD – power spectral density
sEEG – intracranial stereotactic electroencephalography
CGSA – coarse graining spectral analysis

Funding sources

Authors have not received any funding for this article preparation.

Declaration of generative AI in scientific writing

During the preparation of this work the authors did not use any generative AI tools or services.

Data statement

All data are publicly available at: https://mni-open-ieegatlas.research.mcgill.ca/main.php

Code for the analysis is provided at: https://github.com/armonaite/PowerLawAnalysis.

CRediT authorship contribution statement

Karolina Armonaite: Writing – review & editing, Writing – original draft, Visualization, Validation, Methodology, Formal analysis, Conceptualization. **Livio Conti:** Writing – review & editing, Writing – original draft, Validation, Supervision, Methodology, Investigation, Conceptualization. **Marco Balsi:** Writing – review & editing. **Luca Paulon:** Writing – review & editing. **Franca Tecchio:** Writing – review & editing, Writing – original draft, Validation, Methodology.

Declaration of competing interest

The authors declare that they have no known competing financial interests or personal relationships that could have appeared to influence the work reported in this paper.

Acknowledgments

We are grateful for those who made this intracranial electroencephalography data publicly available.

Supplementary materials

Supplementary material associated with this article can be found, in the online version, at doi:10.1016/j.physd.2025.134733.

Data availability

We have used data publically available and we provide the link in the manuscript.

References

[1] A. Clauset, C.R. Shalizi, M.E.J. Newman, Power-law distributions in empirical data, SIAM Rev 51 (2009) 661–703.
[2] G. Werner, Fractals in the nervous system: conceptual implications for theoretical neuroscience, Front. Physiol. 1 JUL (2010).
[3] A. Di Ieva, F. Grizzi, H. Jelinek, A.J. Pellionisz, G.A. Losa, Fractals in the neurosciences, part I: general principles and basic neurosciences, Neuroscientist 20 (2014) 403–417.
[4] E. Olejarczyk, J. Gotman, B. Frauscher, Region-specific complexity of the intracranial EEG in the sleeping human brain, Sci. Rep. 12 (2022).
[5] G. Lima-Mendez, J. Van Helden, The powerful law of the power law and other myths in network biology, Mol. Biosyst. 5 (2009) 1482–1493.
[6] G. Buzsaki, K. Mizuseki, The log-dynamic brain: how skewed distributions affect network operations, Nat Rev Neurosci 15 (2014) 264–278.
[7] A.D. Broido, A. Clauset, Scale-free networks are rare, Nat Commun 10 (2019).
[8] A. Eke, P. Herman, L. Kocsis, L.R. Kozak, Fractal characterization of complexity in temporal physiological signals, Physiol. Meas. 23 (2002).
[9] Ivanov, P.C., Amaral, A.N. & Stanley, H.E. Multifractality in human heartbeat dynamics. 399, 461–465 (1999).
[10] O. Adriani, et al., PAMELA measurements of cosmic-ray proton and helium spectra, Science (80-.) 332 (2011) 69–72.
[11] Z.E. Ross, D.T. Trugman, E. Hauksson, P.M Shearer, Searching for hidden earthquakes in Southern California, Science (80-.) 6888 (2019).
[12] C.M.A. Pinto, A. Mendes Lopes, J.A.T. Machado, A review of power laws in real life phenomena, Commun. Nonlinear Sci. Numer. Simul. 17 (2012) 3558–3578.
[13] Ivanov, P.C. et al. From 1 /f noise to multifractal cascades in heartbeat dynamics From 1 Ò f noise to multifractal cascades in heartbeat dynamics. 641, (2012).
[14] L.J. Fosque, R.V. Williams-garcía, J.M. Beggs, G. Ortiz, Evidence for quasicritical brain dynamics, Phys. Rev. Lett. 126 (2021) 98101.
[15] D.L. Gilden, T. Thornton, M.W. M. 1/f noise in Human cognition. 267, 1837–1840 (1995).
[16] S.A. Jones, J.H. Barfield, V.K. Norman, W.L. Shew, Scale-free behavioral dynamics directly linked with scale-free cortical dynamics, Elife 12 (2023) 1–23.
[17] G.-C. Flores-Marquez, N. C, Fractal dimension analysis of the magnetic time series associated with the volcanic activity of Popocatépetl, Nonlinear Process Geophys (2012) 693–701, https://doi.org/10.5194/npg-19-693-2012.
[18] S. Kesić, S.Z. Spasić, Application of Higuchi's fractal dimension from basic to clinical neurophysiology: a review, Comput. Methods Programs Biomed. 133 (2016) 55–70.
[19] H. Wen, Z. Liu, Separating fractal and oscillatory components in the power spectrum of neurophysiological signal, Brain Topogr 29 (2016) 13–26.
[20] Fries, P. Neuronal gamma-band synchronization as a fundamental process in cortical computation. https://doi.org/10.1146/annurev.neuro.051508.135603 32, 209–224 (2009).
[21] J. Samaha, M.X. Cohen, Power spectrum slope confounds estimation of instantaneous oscillatory frequency, Neuroimage 250 (2022) 118929.
[22] B.J. He, Scale-free brain activity: past, present, and future, Trends Cogn. Sci. (Regul. Ed.) 18 (2014) 480–487.
[23] G. Buzsáki, A. Draguhn, Neuronal olscillations in cortical networks, Science 304 (2004) 1926–1929.
[24] R. Evertz, D.G. Hicks, D.T.J. Liley, Alpha blocking and 1/fβ spectral scaling in resting EEG can be accounted for by a sum of damped alpha band oscillatory processes, PLoS Comput. Biol. 18 (2022).
[25] Kantelhardt, J.W. et al. Multifractal detrended uctuation analysis of nonstationary time series. 316, 87–114 (2002).
[26] M. Long, et al., Room temperature high-detectivity mid-infrared photodetectors based on black arsenic phosphorus, Sci. Adv. 3 (2017) 1–8.
[27] B.J. He, J.M. Zempel, A.Z. Snyder, M.E. Raichle, The temporal structures and functional significance of scale-free brain activity, Neuron 66 (2010) 353–369.
[28] D. La Rocca, N. Zilber, P. Abry, V. van Wassenhove, P. Ciuciu, Self-similarity and multifractality in human brain activity: a wavelet-based analysis of scale-free brain dynamics, J. Neurosci. Methods 309 (2018) 175–187.
[29] T. Donoghue, et al., Parameterizing neural power spectra into periodic and aperiodic components, Nat. Neurosci. 23 (2020) 1655–1665.
[30] Z.G. Nicolaou, M. Sebek, I.Z. Kiss, A.E. Motter, Coherent dynamics enhanced by uncorrelated noise, Phys. Rev. Lett. 125 (2020) 94101.
[31] R.F. Helfrich, J.D. Lendner, R.T. Knight, Aperiodic sleep networks promote memory consolidation, Trends Cogn. Sci. 25 (2021) 648–659.
[32] P. Allegrini, et al., Spontaneous brain activity as a source of ideal 1/f noise, Phys. Rev. E - Stat. Nonlinear, Soft Matter Phys. 80 (2009) 1–13.
[33] Akbarian, F., Rossi, C., Costers, L. & Marie, B.D. Stimulus-related modulation in the 1 /f spectral slope suggests an impaired inhibition of irrelevant information in people with multiple sclerosis. 1–35 (2023).
[34] N. Kannathal, U.R. Acharya, C.M. Lim, P.K. Sadasivan, Characterization of EEG - A comparative study, Comput. Methods Programs Biomed. 80 (2005) 17–23.
[35] Acharya U., R., Faust, O., Kannathal, N., Chua, T. & Laxminarayan, S. Non-linear analysis of EEG signals at various sleep stages. 80, 37–45 (2005).

[36] P. Croce, A. Quercia, S. Costa, F. Zappasodi, Circadian rhythms in fractal features of EEG signals, Front. Physiol. 9 (2018) 1567.
[37] D.M. Hernán, et al., Order and chaos in the brain: fractal time series analysis of the EEG activity during a cognitive problem solving task, Procedia Comput. Sci. 55 (2015) 1410–1419.
[38] A. Pascarella, et al., Normalized compression distance to measure cortico-muscular synchronization, Front. Neurosci. 16 (2022).
[39] M.R. Pagliara, et al., On the homology of the dominant and non-dominant corticospinal tracts: a novel neurophysiological assessment, Brain Sci 13 (2023) 278. *2023, Vol. 13, Page 278*.
[40] A.H. Al-Nuaimi, E. Jammeh, L. Sun, E. Ifeachor, Higuchi fractal dimension of the electroencephalogram as a biomarker for early detection of Alzheimer's disease, in: Proc. Annu. Int. Conf. IEEE Eng. Med. Biol. Soc. EMBS, 2017, pp. 2320–2324, https://doi.org/10.1109/EMBC.2017.8037320.
[41] K. Armonaite, et al., Neuronal electrical ongoing activity as cortical areas signature: an insight from MNI intracerebral recording atlas, Cereb. Cortex (2021).
[42] R. Sharma, R.B. Pachori, Classification of epileptic seizures in EEG signals based on phase space representation of intrinsic mode functions, Expert Syst. Appl. 42 (2015) 1106–1117.
[43] T. L'Abbate, et al., Corticomuscular coherence dependence on body side and visual feedback, Neuroscience 490 (2022) 144–154.
[44] Y.-C. Lai, D. Lerner, Effective scaling regime for computing the correlation dimension from chaotic time series, Phys. D 115 (1998) 1–18.
[45] S. Spasić, A. Kalauzi, M. Ćulić, G. Grbić, L. Martać, Estimation of parameter kmax in fractal analysis of rat brain activity, Ann. N. Y. Acad. Sci. 1048 (2005) 427–429.
[46] Cannon, M.J., Percival, D.B., Caccia, D.C., Raymond, G.M. & Bassingthwaighte, J. B. Evaluating scaled windowed variance methods for estimating the Hurst coefficient of time series. 241, 606–626 (1997).
[47] Katsev, S. & Heureux, I.L. Are Hurst exponents estimated from short or irregular time series meaningful? 29, 1085–1089 (2003).
[48] B. Frauscher, et al., Atlas of the normal intracranial electroencephalogram: neurophysiological awake activity in different cortical areas, Brain 141 (2018) 1130–1144.
[49] N. von Ellenrieder, et al., How the Human brain sleeps: direct cortical recordings of normal brain activity, Ann. Neurol. 87 (2020) 289–301.
[50] K. Armonaite, et al., Local neurodynamics as a signature of cortical areas: new insights from sleep, Cereb. Cortex 33 (2023) 3284–3292.
[51] Zimmern, V. Why brain criticality is clinically relevant : a scoping review. 14, 1–34 (2020).
[52] R.E. Welsch, Robust regression using iteratively reweighted least-squares, Commun. Stat. - Theory Methods 6 (1977) 813–827.
[53] H. Abdi, L.J. Williams, Honestly significant difference (HSD) test, Encycl. Res. Des. 1–5 (2010), https://doi.org/10.4135/9781412961288.n181.
[54] A. Ikeda, H.O. Lüders, R.C. Burgess, H. Shibasaki, Movement-related potentials recorded from supplementary motor area and primary motor area: role of supplementary motor area in voluntary movements, Brain 115 (1992) 1017–1043.
[55] M.M. Schartner, et al., Global and local complexity of intracranial EEG decreases during NREM sleep, Neurosci. Conscious. 2017 (2020) 1–12.
[56] E. Bullmore, O. Sporns, The economy of brain network organization, Nat. Rev. Neurosci. 13 (2012) 336–349. *2012 135*.
[57] Craddock, R.C., James, G.A., Holtzheimer, P.E., Hu, X.P. & Mayberg, H.S. A whole brain fMRI atlas generated via spatially constrained spectral clustering. 00, (2011).
[58] Arslan, S., Makropoulos, A., Robinson, E.C., Rueckert, D. & Parisot, S. NeuroImage Human brain mapping : a systematic comparison of parcellation methods for the human cerebral cortex. 170, 5–30 (2018).
[59] A. Keitel, J. Gross, Individual Human brain areas can Be identified from their characteristic spectral activation fingerprints, PLoS Biol. 14 (2016).
[60] C. Cottone, et al., Neuronal electrical ongoing activity as a signature of cortical areas, Brain Struct. Funct. 222 (2017) 2115–2126.
[61] S.D. Muthukumaraswamy, D.T. Liley, 1/F electrophysiological spectra in resting and drug-induced states can Be explained by the dynamics of multiple oscillatory relaxation processes, Neuroimage 179 (2018) 582–595.
[62] C.-K. Peng, S.V. Buldyrev, S. Havlin, M. Simons, H.E. Stanley, A.L. G, Mosaic organization of DNA nucleotides, Phys. Rev. E 330 (1994) 1527–1530.
[63] N. Xu, P. Shang, S. Kamae, Minimizing the effect of exponential trends in detrended fluctuation analysis, Chaos, Solitons and Fractals 41 (2009) 311–316.
[64] Y. Yamamoto, R.L. Hughson, Coarse-graining spectral analysis: new method for studying heart rate variability, J. Appl. Physiol. 71 (1991) 1143–1150.
[65] W.J. Freeman, J. Zhai, Simulated power spectral density (PSD) of background electrocorticogram (ECoG), Cogn. Neurodyn. 3 (2009) 97–103.
[66] K.J. Miller, L.B. Sorensen, J.G. Ojemann, M.den Nijs, ower-Law scaling in the brain surface electric potential, PLoS Comput. Biol. (12) (2009). Plos Computational Biology.
[67] Hodkinson et al. Scale-free amplitude modulation of low-frequency fluctuations in episodic Migraine _ Enhanced reader.Pdf. (2019).
[68] E.J. Peterson, B.Q. Rosen, A.M. Campbell D, A. Belger, B. Voytek, 1/F neural noise is a better predictor of schizophrenia than neural oscillations, bioRxiv 113449 (2018).
[69] O. Vyšata, et al., Change in the characteristics of EEG color noise in alzheimer's disease, Clin. EEG Neurosci. 45 (2014) 147–151.
[70] J.M. Hausdorff, C.K. Peng, Multiscaled randomness: a possible source of 1/f noise in biology, Phys. Rev. E - Stat. Physics, Plasmas, Fluids, Relat. Interdiscip. Top. 54 (1996) 2154–2157.
[71] G. Buzsáki, Rhythms of the brain, Rhythms of the Brain (2009), https://doi.org/10.1093/acprof:oso/9780195301069.001.0001.
[72] Beggs, J.M. & Plenz, D. Neuronal avalanches in neocortical circuits. 23, 11167–11177 (2003).
[73] D.P. Almond, B. Vainas, The electrical characteristics of random RC networks and the physical origin of 1 /f noise The electrical characteristics of random RC networks and the physical origin of 1 / f noise, J. Phys. Condens. Matter 1 (2001).
[74] C. Bédard, H. Kröger, A. Destexhe, Does the 1/f frequency scaling of brain signals reflect self-organized critical states? Phys. Rev. Lett. 97 (2006) 1–4.
[75] G. Barbati, et al., Functional source separation from magnetoencephalographic signals, Hum. Brain Mapp. 27 (2006) 925–934.